Geomechanics and Engineering, *Vol. 31, No. 5 (2022) 505-518*
https://doi.org/10.12989/gae.2022.31.5.505

Modified *p-y* curves to characterize the lateral behavior of helical piles

Hyeong-Joo Kim[1a], James Vincent Reyes[*2], Peter Rey Dinoy[2b], Tae-Woong Park[3c], Hyeong-Soo Kim[2d] and Jun-Young Kim[2e]

[1]Department of Civil Engineering, Kunsan National University, 558 Daehak-ro, Miryong-dong, Gunsan 54150, Republic of Korea
[2]Department of Civil and Environmental Engineering, Kunsan National University, 558 Daehak-ro, Miryong-dong, Gunsan 54150, Republic of Korea
[3]Renewable Energy Research Institute, Kunsan National University, 558 Daehak-ro, Miryong-dong, Gunsan 54150, Republic of Korea

(*Received August 26, 2021, Revised September 30, 2022, Accepted November 24, 2022*)

Abstract. This study introduces soil resistance multipliers at locations encompassed by the zone of influence of the helix plate to consider the added lateral resistance provided to the helical pile. The zone of influence of a helix plate is a function of its diameter and serves as a boundary condition for the modified soil resistance springs. The concept is based on implementing p-multipliers as a reduction factor for piles in group action. The application of modified *p-y* springs in the analysis of helical piles allows for better characterization and understanding of the lateral behavior of helical piles, which will help further the development of design methods. To execute the proposed method, a finite difference program, HPCap (Helical Pile Capacity), was developed by the authors using Matlab. The program computes the deflection, shear force, bending moment, and soil resistance of the helical pile and allows the user to freely input the value of the zone of influence and Ω (a coefficient that affects the value of the *p*-multiplier). Results from ten full-scale lateral load tests on helical piles embedded at depths of 3.0 m with varying shaft diameters, shaft thicknesses, and helix configurations were analyzed to determine the zone of influence and the magnitude of the p-multipliers. The analysis determined that the value of the p-multipliers is influenced by the ratio between the pile embedment length and the shaft diameter (D_p), the effective helix diameter (D_h-D_p), and the zone of influence. Furthermore, the zone of influence is recommended to be 1.75 times the helix diameter (D_h). Using the numerical analysis method presented in this study, the predicted deflections of the various helical pile cases showed good agreement with the observed field test results.

Keywords: finite difference method; helical piles; lateral load test; *p*-multiplier; *p-y* springs

1. Introduction

Photovoltaic power generation is currently on the rise and sought-after around the world due to its inexhaustible and non-polluting resource which emphasizes the vision of sustainable development. Shallow foundations, due to their design feature of having a wide base, are excellent to transmit and distribute the structural loads of these renewable energy systems to the supporting soil. But due to the use of mass concrete, they create environmental concerns and may not perform well in soft soils that are prone to tilting due to differential settlement. Another issue presents itself as high uplift forces from subsequent wind loading. With this taken into consideration, an alternative solution is through helical pile foundations.

According to Lutenegger (2011), helical piles were one of the most globally important engineering advances introduced during the 19th century as a practical foundation system. As shown in Fig. 1, a helical pile consists of one or more helix plates spaced at specified intervals welded to the central pile shaft. Historically these have mainly been used for lighthouses and transmission towers due to their unprecedented axial capacity compared to the traditional single straight-shafted counterpart. Spagnoli *et al.* (2015) and Davidson *et al.* (2022) described its ease of installation and removal, making it a potential alternative to driven piles, especially regarding the marine environment, due to the various environmental concerns associated with pile driving and overall operational noise. Vignesh and Mayakrishnan (2020) describe its convenient and economical usage where field soil conditions have a high groundwater table.

Numerous studies have been carried out globally on the behavior of helical piles exposed to axial loads, and considerable research on lateral loading is present in the literature. As mentioned by Lee *et al.* (2019), piles exposed to lateral loads experience greater moments than those axially loaded, thus constituting an in-depth examination. Among the established researchers are Prasad and Rao (1996) and Sakr (2009, 2018), who investigated the lateral capacity embedded in clay soils, Mittal *et al.* (2010) and Abdrabbo and Wakil (2016) studied the static equilibrium

*Corresponding author, Graduate Student
E-mail: james17@kunsan.ac.kr
[a]Professor
[b]Ph.D.
[c]Ph.D.
[d]Ph.D.
[e]Graduate Student

http://www.techno-press.org/?journal=gae&subpage=7
ISSN: 2005-307X (Print), 2092-6219 (Online)

Fig. 1 Typical geometry of a helical pile

of helical piles and performed tests on a physical model in cohesionless soils, and Zhang (1999) carried out in-situ lateral load tests in both clay and sand. A common conclusion was reached that it exhibits more excellent lateral resistance due to the presence of helices compared to traditional single straight-shafted piles by observing its lateral displacement. Despite the various research accounts about its lateral resistance, the lack of proper design criteria has impaired the confidence in using helical piles for large-scale infrastructure projects, especially in liquefiable soils, as mentioned by Kim *et al.* (2020, 2021).

The *p-y* curve approach is widely used for characterizing the behavior of laterally loaded piles documented by various researchers such as Matlock (1970), Welch and Reese (1972), Reese *et al.* 1974, Reese (1997), Crowther (1990), Foriero *et al.* (2005), Shelman *et al.* (2014), Li and Yang (2017), and Lim and Jeong (2018). Currently, the study conducted by Elkasabgy and El Naggar (2019) is the only available reference material documenting the lateral performance of a helical pile using the *p-y* approach. They conducted five large-scale helical pile tests in clayey glacial deposits with single and double helix configurations with embedment ratios (H/D) ranging from 6.0 to 13.9. The researchers concluded that the lateral behavior of the tested helical piles was controlled generally by the shaft resistance and the helical plates' contribution was negligible. From their research findings, it was shown that the location where the helices are crucial to the additional lateral soil resistance that can be provided.

A numerical study using finite element analysis (FEM) conducted by Al-Baghdadi *et al.* (2015, 2017) suggests that helices (or flanges as they refer to them) installed near the mud-line produce a moderate contribution to the lateral resistance and the presence of compressive axial loads on the pile increases lateral capacity while uplift loads reduce it marginally.

To simulate the behavior of a helical pile under axial and lateral loading, the authors developed the finite difference program HPCap (Helical Pile CAPacity) based on the load transfer method using Matlab vR2021a. The program uses 100 and 500 nodes to accurately predict the behavior of the pile element under axial and lateral loading, respectively. The nodes are replaced by springs, utilizing load transfer curves to represent the soil resistance provided by the shaft, helix, and tip. To account for the compressive and uplift resistance contributed by the helix, the program employs a load transfer curve derived from experiments conducted on large-capacity helical piles. For the lateral analysis, the program generates *p-y* curves based on recommendations from the literature for various types of soils to represent soil resistance from the shaft. At the location of the helices, HPCap introduces *p-multipliers* to consider the added lateral resistance provided by the helix. The concept of p-multipliers was initially used as a reduction factor for piles in-group action in the research study conducted by Fayyazi *et al.* (2012). The main difference in this study compared to the other recorded studies is that the first helix is stationed as close as possible to the ground level. Verification of the coded program is done by comparing the results with the commercial LPile program. LPile is a computer program developed and licensed by Ensoft Inc that specializes in the analysis of laterally loaded piles employing the *p-y* method. Validation of the numerical analysis solution is achieved by comparing the predicted results versus the full-scale test data. Installation effects are not considered in this study.

2. Theoretical background

The evaluation of piles under lateral loading is one of the frequent problems of soil-structure interaction prevalent in the field of civil engineering. The soil resistance at any point along the embedded pile length is a function of pile deflection and vice versa. This complex soil-structure interaction problem requires the supplementation of a numerical procedure based on the concept of an elastic beam on a deformable foundation, commonly known as the Winkler foundation. This method is preferred over simplistic methodologies owing to its ability to predict pile displacements, as noted by various technical procedures and researchers such as Japan Road Association (2002), Haigh (2002), Haigh and Madabhushi (2002), Dobry *et al.* (2003), Gonzales *et al.* (2005), and He *et al.* (2009) and over more complex methods such as the finite element method (FEM) due to its dependency on the constitutive model's reliability as mentioned by Li and Dafalias (2000), Finn and Thavaraj (2001), Yang *et al.* (2003), Lam *et al.* (2009) and Cheng and Jeremic (2009). The pile is idealized as an embedded beam-column element connected to the surrounding soil discretized as non-linear springs. The behavior of one spring does not affect any adjacent spring, as each spring acts independently. The solution involves three critical conditions: (a) solution to the fourth-order differential equation, (b) selection of appropriate *p-y* model based on soil type, and most importantly, (c) reliability of input soil parameters.

2.1 The fourth-order differential equation

Hetenyi (1946) presented the derivation of the differential equation for the beam-column foundation shown in Eq. (1). The assumption is based on the structural equilibrium of a beam-column element inserted on an elastic foundation and subjected to horizontal loading and a pair of compressive forces acting at the centroid of the end of the cross-section.

$$EI\frac{d^4y}{dx^4} + P_x\frac{d^2y}{dx^2} + E_s y = q \tag{1}$$

where EI is the flexural rigidity of the pile material, P_x is the axial load on the pile, q is the uniformly distributed vertical load on the beam, and p is the soil resisting pressure along pile length.

The basic relationships from the differential equation can be written as shown through Eqs. (2)-(6)

Slope

$$S = \frac{dy}{dx} \tag{2}$$

Moment

$$M = EI\frac{d^2y}{dx^2} \tag{3}$$

Shear

$$V = \frac{dM}{dx} = EI\frac{d^3y}{dx^3} \tag{4}$$

Uniformly distributed load

$$q = \frac{dV}{dx} = EI\frac{d^2M}{dx^2} = EI\frac{d^4y}{dx^4} \tag{5}$$

Soil resisting pressure

$$p = -E_s y \tag{6}$$

where E_s is the soil modulus and y is the deflection along the pile length

2.2 Solution to the fourth-order differential equation

The solution is based on the finite difference approach, which requires two main criteria to be satisfied in order to proceed: (a) the general differential equation approximation and (b) the set of boundary conditions.

Gleser (1953) first suggested the finite difference approach for the solution of laterally loaded piles, which numerous researchers, including Reese and Matlock (1956) and Matlock (1960), then extended the idea. The solution requires the derivation of central difference approximations for the elastic curve of the deflected shape. The slope of the elastic curve is approximated to be a secant drawn through two points adjacent to the curve, as shown in Fig. 2.

The general differential equation from Eq. (1) in finite difference form is displayed in Eq. (7)

$$\begin{gathered} y_{(i+2)}\left[R_{(i+1)}\right] + y_{(i+1)}\left[-2R_{(i+1)} - 2R_i + P_x h^2\right] \\ +y_i\left[R_{(i+1)} + 4R_i + R_{(i-1)} + 2P_x h^2 + E_{si}h^4\right] \\ +y_{(i-1)}\left[-2R_i - 2R_{(i-1)} + P_x h^2\right] + \\ y_{(i-2)}\left[R_{(i-1)}\right] - qh^4 = 0 \end{gathered} \tag{7}$$

where R is the flexural rigidity of the pile cross-section (EI), h is the distance between the two adjacent points and the other variables are as defined before.

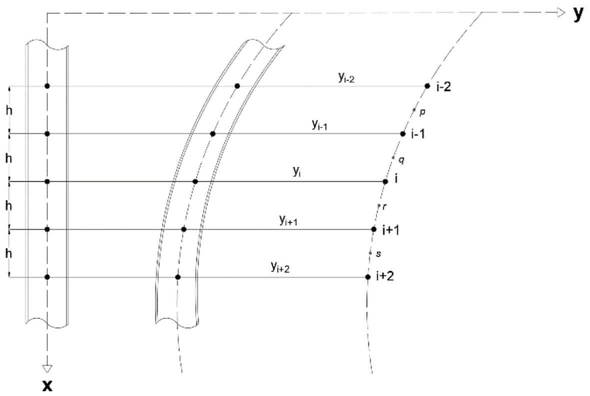

Fig. 2 Geometric basis for the central difference approximations

Since the general equation is in the fourth order in terms of dependent variable y, four boundary conditions are required. A set of simultaneous equations are then formulated, which yields the deflected shape of the pile. If deflection values are found, moment, shear, and soil resistance can be obtained for any location along the pile by using back substitution of appropriate values into appropriate equations.

For a more comprehensive and detailed discussion of the solution, refer to the technical report done by Reese *et al.* (1984).

2.3 Formulation of a typical p-y curve

A key component to accurately defining the behavior of a laterally loaded pile foundation is using *p-y* curves noted by various authors such as Bouzid *et al.* (2013) and Kim *et al.* (2015). A typical *p-y* curve describes the non-linear relationship between the soil resistance and the lateral deflection of the embedded structural element. The synthesis of *p-y* curves was based on the results of instrumented full-scale experiments conducted by researchers such as Matlock (1970) and Welch and Reese (1972). The supporting medium, which is the soil, is classified into three major types: clay, sand, and rock, where each has its own parameters and non-linear curves to describe the load-displacement behavior.

For sandy soils, the case study conducted by Reese *et al.* (1974) at Mustang Island is the basis of *p-y* curves for static and cyclic loading. Their procedure accounts for sandy soils with the presence of water above or below the water table. The crucial soil parameters required for sandy soils are the best estimates of (a) friction angle, ϕ and (b) soil unit weight, γ (for soils below water table, the effective unit weight must be used; while for soil above the water table, the total unit weight).

Preliminary computations are done using Eqs. (8)-(11). For soil resistance at any depth of the pile-embedded length, the depth of intersection between Eqs. (12) and (13) is required. Setting both equations equal, the intersection depth, z_t, is obtained. For depths less than the intersection depth, the soil resistance is obtained using Eq. (12), while Eq. (13) is used for depths greater than the intersection value. A typical *p-y* curve for sandy soils subject to static loading increases in magnitude per depth, as shown in Fig. 3.

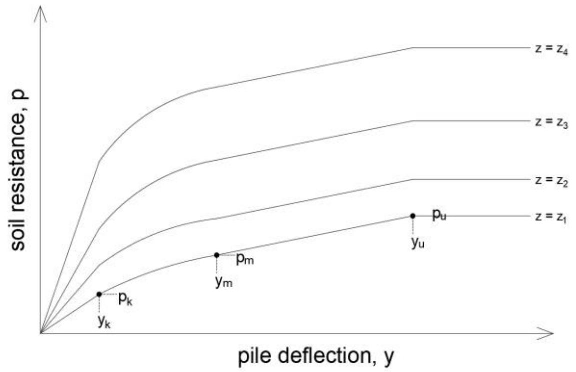

Fig. 3 Characteristic shape of a *p*-*y* curve for sandy soils

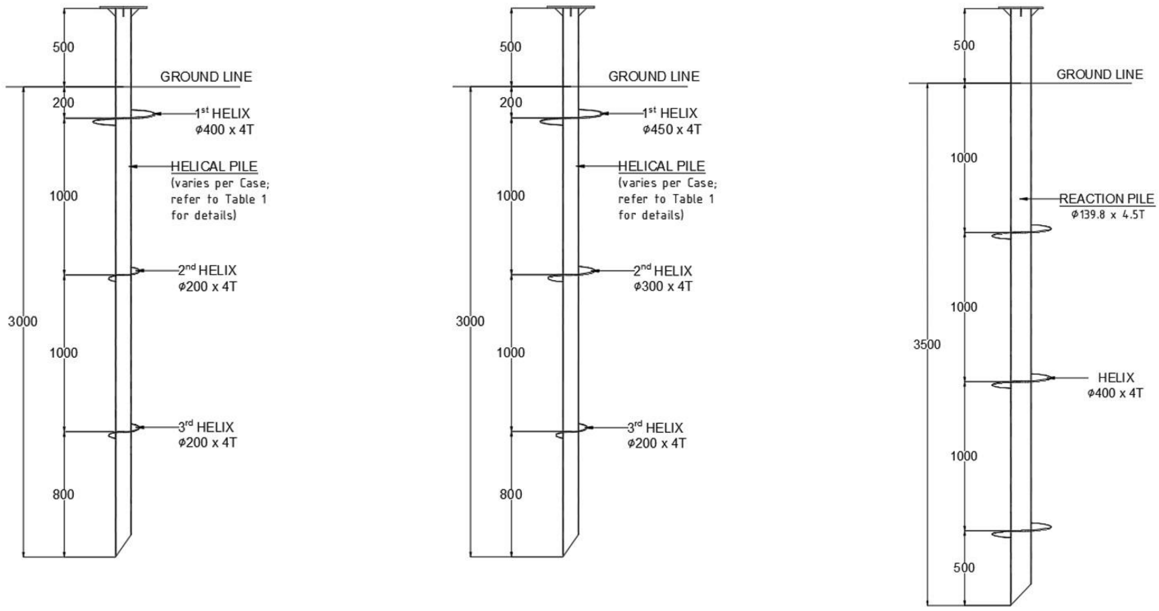

(a) Helix Configuration 1 (400-200-200)

(b) Helix Configuration 2 (450-300-200)

(c) Reaction Pile

Fig. 4 Diagram of helical piles for testing (a and b) and reaction pile (c)

$$\alpha = \frac{\phi}{2} \tag{8}$$

$$\beta = 45 + \frac{\phi}{2} \tag{9}$$

$$K_0 = 0.4 \tag{10}$$

$$K_a = \tan^2\left(45 - \frac{\phi}{2}\right) \tag{11}$$

$$P_{st} = \gamma z \begin{bmatrix} \dfrac{K_0 z \tan\phi \sin\beta}{\tan(\beta - \phi)\cos\alpha} \\ + \dfrac{\tan\beta}{\tan(\beta-\phi)}(b + z\tan\beta\tan\alpha) \\ + K_0 z \tan\beta(\tan\phi\sin\beta - \tan\alpha) - K_a b \end{bmatrix} \tag{12}$$

$$P_{sd} = K_a b\gamma z(tan^8\beta - 1) + K_0 b\gamma z\, tan^4\beta \tag{13}$$

3. Full scale load tests

Full-scale lateral load tests were performed at the 300 MW Onshore Solar Power Generation Project located in the Saemangeum area of the Jeollabuk-do province of South Korea. Helical test piles consisted of three different pile diameters (89.1 mm, 101.6 mm, and 114.3 mm), two wall thicknesses (3.2 mm and 4.0 mm), and two types of helices configuration (400-200-200 and 450-300-200) totaling of 10 experimental cases, further details are shown in Table 1. These helical piles were installed onto the ground using a commercially available hydraulic driver mounted on a mini CAT excavator. The vertical penetration rate for all cases was controlled at 0.1 m increments which correspond to the pitch length of the helix plate.

The steel material used in manufacturing the helical pile and its helices has a yield strength of 355 MPa. As shown in Figs. 4(a) and 4(b), the helical piles have an embedded

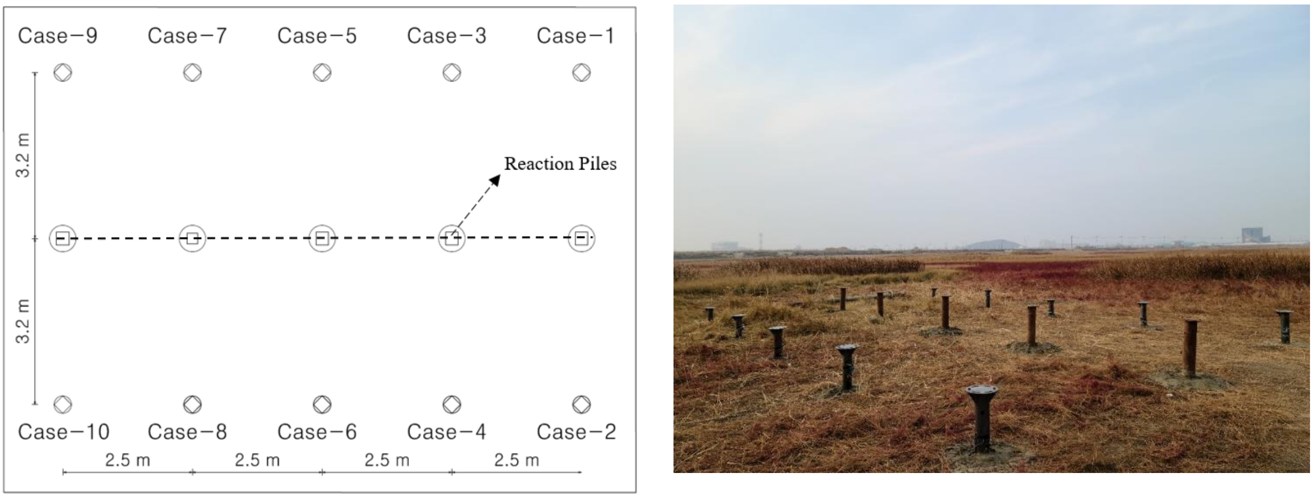

(a) Plan view (b) Field view

Fig. 5 Layout of reaction piles and the 10 helical piles for load testing

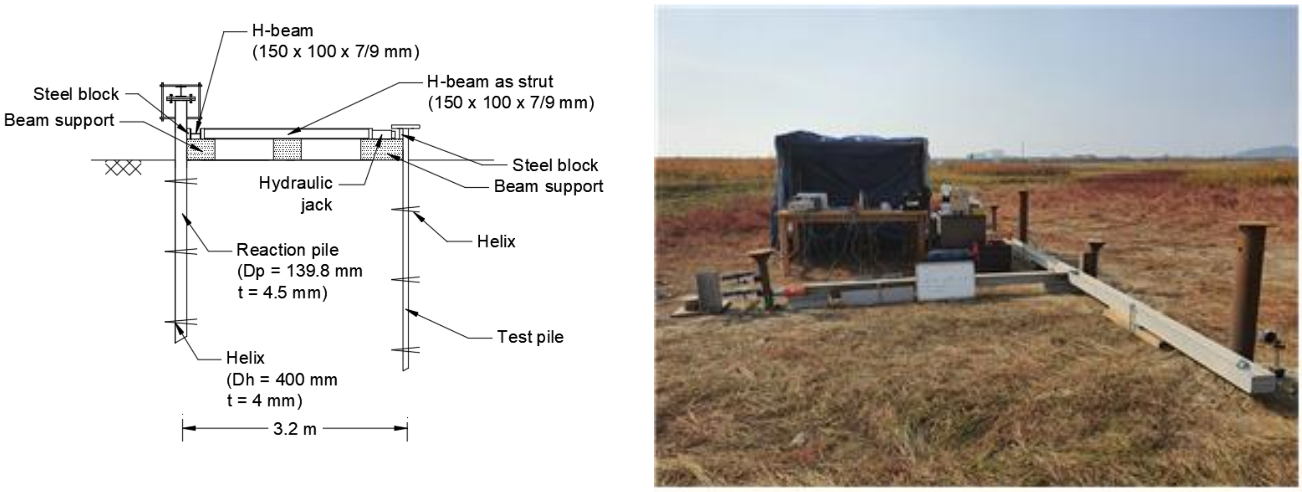

(a) Plan view (b) Field view

Fig. 6 Layout of load test for helical piles

length of 3 m with a protruding 0.5 m portion for a total length of 3.5 m. The helices have a thickness of 4mm and are welded to the central shaft; the first helix is located 0.2 m below the ground level, and succeeding helices are spaced 1 m apart. Reaction piles have a similar length to the helical piles with a central shaft diameter of 139.8 mm and a thickness of 4.5 mm fitted with 3-400 mm diameter helices with 4 mm thickness; the first helix is located 1 m below ground level, and the succeeding helices are spaced at 1 m intervals along its embedded length as shown in Fig. 4(c). The helical piles were installed in rows parallel to the reaction piles spaced 2.5 m apart center to center and 3.2 m adjacent to the reaction piles as shown in Fig. 5.

As discussed by Zhang *et al.* (1998), the lateral load tests were conducted in accordance with Procedure A (Standard Loading) and in compliance with the technical specifications stated in ASTM D3966-07, Standard Test Methods for Deep Foundations Under Lateral Loading. The typical load test set-up can be seen in Fig. 6. Lateral loads were applied in increments; each increment was maintained for 10-20 minutes for most load steps except for the 200% increment, which was held for 60minutes. A hydraulic jack delivers the load applied on the test pile approximately 0.2 m above ground level connected to an H-beam, which acts as a compression member supported by the reaction pile. The compression member was securely fastened to eliminate the possibility of eccentric loading on the pile surface; the applied load must pass the vertical central axis to avoid warping the shaft section. An electronic load cell with 300 kN capacity was used to monitor the load applied on the test pile. To measure the lateral displacements of the test pile, 2-LVDTs (linear variable differential transformer) with 0.01 mm accuracy and 150 mm travel were connected to an electronic data logger and installed at 0.2 m and 0.4 m on one side of the test pile and the other end connected to an external metal box sturdy enough not to be influenced by the lateral displacements.

Results of the conducted lateral load tests on the 10 cases of helical piles are displayed through Figs. 7-9. As observed throughout the series of tests, the helical piles with

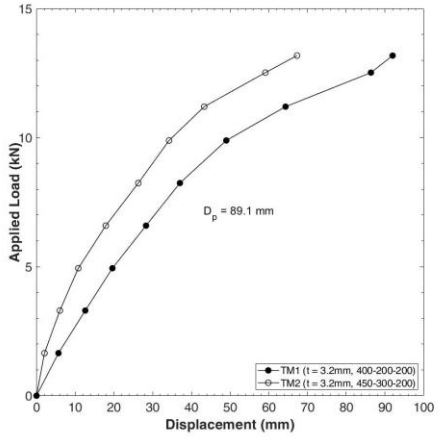

Fig. 7 Field test results for TM1 & TM2

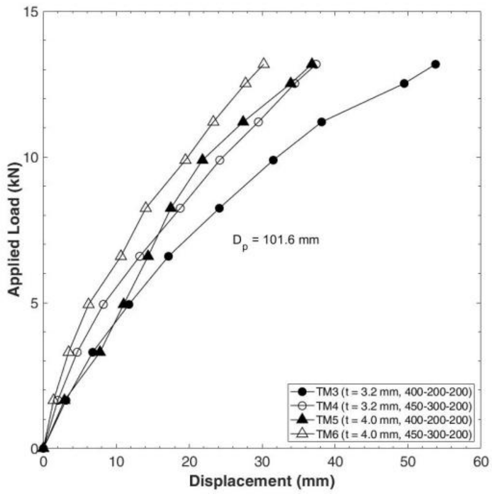

Fig. 8 Field test results for TM3, TM4, TM5 & TM6

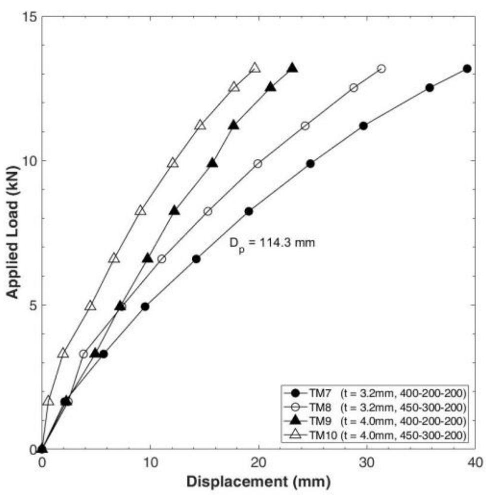

Fig. 9 Field test results for TM7, TM8, TM9 & TM10

helices 450-300-200 mobilized greater lateral resistance compared to the helical pile with only 400-200-200 helices. This establishes that larger helical pile diameters develop lesser pile displacements and greater lateral capacity.

Table 1 Helical test pile data

Case No.	Pile Details	Helix Details
TM1	89.1(D) x 3.2(t) x 3,500(L)	400-200-200 (t=4)
TM2	89.1(D) x 3.2(t) x 3,500(L)	450-300-200 (t=4)
TM3	101.6(D) x 3.2(t) x 3,500(L)	400-200-200 (t=4)
TM4	101.6(D) x 3.2(t) x 3,500(L)	450-300-200 (t=4)
TM5	101.6(D) x 4.0(t) x 3,500(L)	400-200-200 (t=4)
TM6	101.6(D) x 4.0(t) x 3,500(L)	450-300-200 (t=4)
TM7	114.3(D) x 3.2(t) x 3,500(L)	400-200-200 (t=4)
TM8	114.3(D) x 3.2(t) x 3,500(L)	450-300-200 (t=4)
TM9	114.3(D) x 4.0(t) x 3,500(L)	400-200-200 (t=4)
TM10	114.3(D) x 4.0(t) x 3,500(L)	450-300-200 (t=4)

4. Geotechnical properties at research area

The research area shown in Fig. 10(a) corresponds to the Saemangeum area of the Jeollabuk-do province of South Korea, where the site was once a coastal area in the past but changed through numerous reclamation projects of coastal lowlands that heavily influenced the change in overall topography. The test bed designated as TB-2, as shown in Fig. 10(b), is nearby boreholes BB-6, BB-7, and BB-8, where SPT (Standard Penetration Test), CPT-1 (Cone Penetration Test), and SST-1 (Swedish Sounding Test) were conducted. SPT was conducted in accordance with the Korean Industrial Standard (KS F 2307), where samples were collected using the Split Spoon Sampler at 1m regular intervals up to a penetration depth of 30 m, shown in Fig 11(a). For the Swedish Sounding Test, data were collected for every 0.25m penetration up to a depth of 5 m, shown in Fig. 11(b). Lastly, CPT was conducted with a 20 mm/s rate of penetration up to a depth of 10.3m as shown in Figs. 11(c) and 11(d). Sieve analysis for boreholes BB-6, BB-7, and BB-8, with samples from 2.0 and 5.0 m depths, respectively, were also conducted, and results are displayed in Fig. 12.

From the in-situ tests, the ground level to an average depth of 3.8 m indicates a layer of loose saturated sand mixtures (silty sand). The area near the test bed was also noted to have the presence of small cobbles during the visual inspection. Weighing the advantages and disadvantages of the tests conducted, the researchers decided to use the SPT test data for the correlation of soil properties to be used in the numerical analysis. Using SPT Correlations Software-NovoSPT, correlations for peak friction angle (ϕ) and saturated unit weight (γ) are obtained and plotted per 1 m depth up to 3 m of penetration to the ground, as shown in Fig. 13. The value taken for hammer correction is 60%, borehole and sampling factor taken as one. Rod length correction factor varies as the depth of penetration increases as well as overburden correction. For friction angle, the method of Hatanaka and Uchida (1996) was selected while, for saturated unit weight, Kulhawy and Mayne (1990).

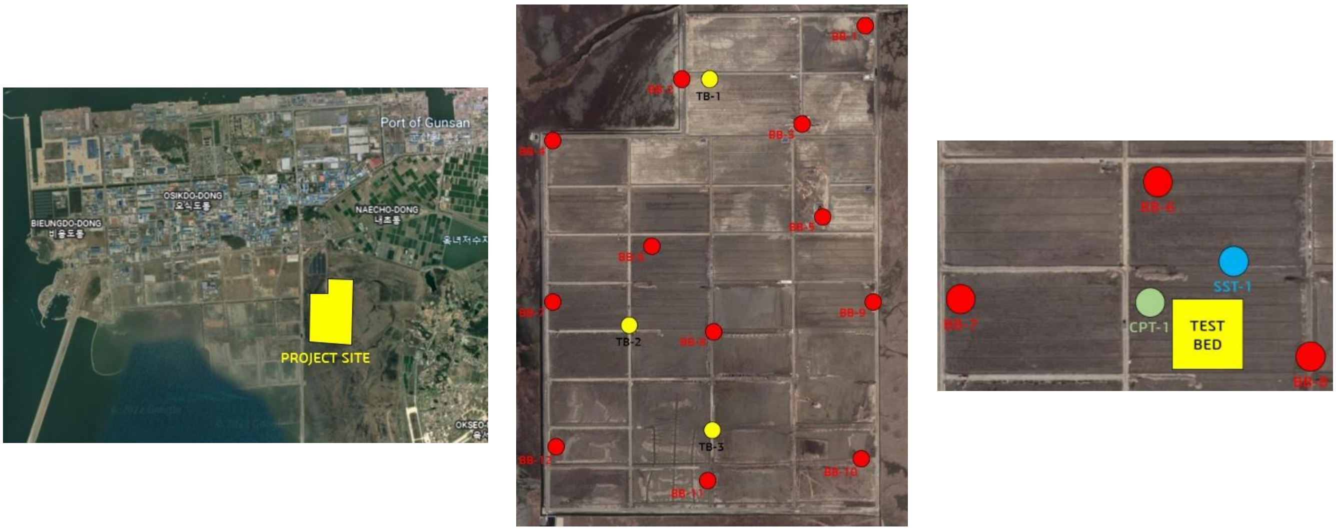

(a) Research area/ project site (300 MW solar power plant)

(b) Boreholes and test bed locations at project site

(c) Location of CPT, SPT and SST relative to test bed

Fig. 10. Test bed details

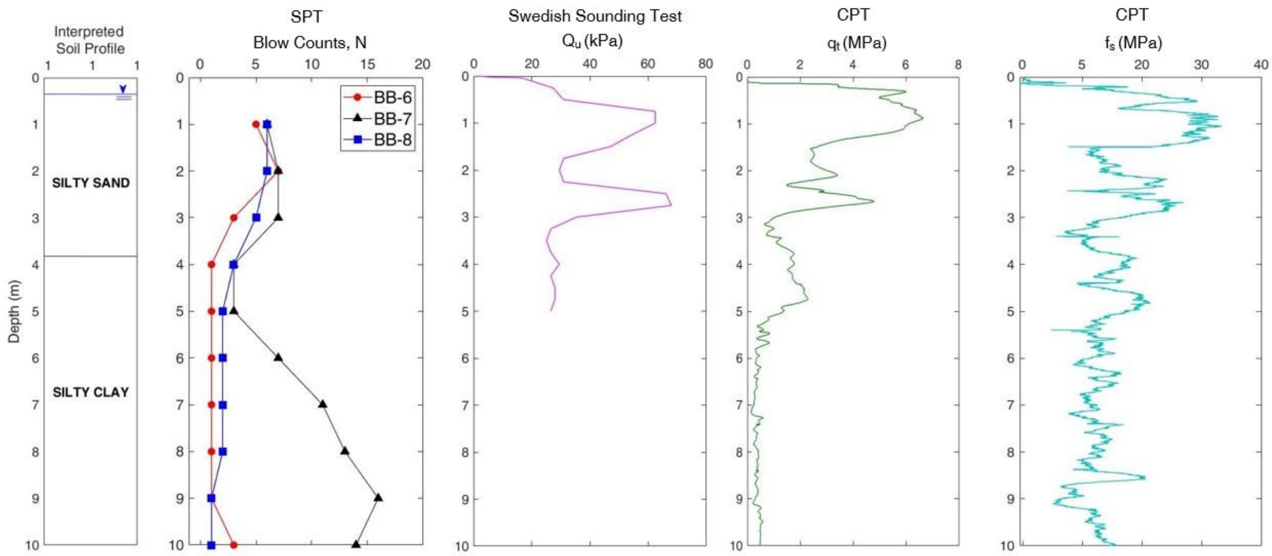

Fig. 11 Collected soil data from various in-situ tests

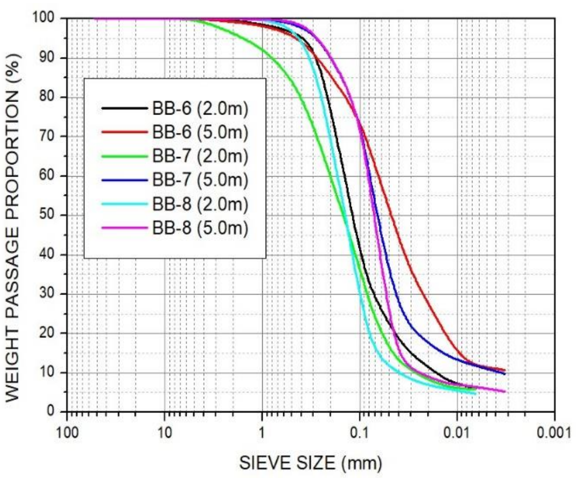

Fig. 12 Particle size distribution curve for BB-6, BB-7 and BB-8

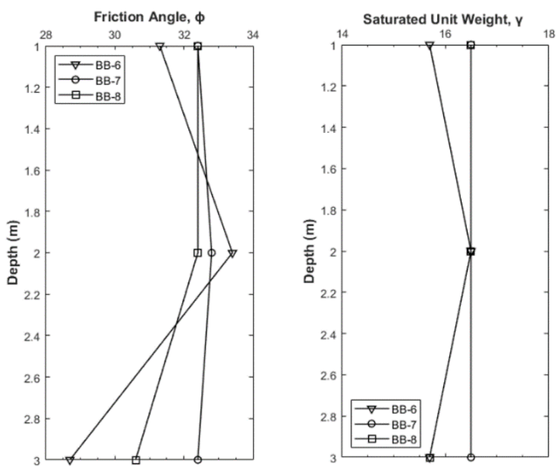

Fig. 13 Correlated soil properties from NovoSPT software

5. Solution to laterally loaded helical piles

To analyze a laterally loaded helical pile, the geotechnical research team of Kunsan National University developed a computer program HPCap (Helical Pile Capacity), for its analysis. The computer program is capable of analyzing both the axial and lateral capacity of the helical pile in multilayered soil (up to five layers) through the modified *p-y* curves concept. The solution method is based on the finite difference method, which utilizes the fourth-order differential equation derived by Hetenyi (1946) and coded using Mathlab vR2021a.

5.1 Verification of solution of laterally loaded piles utilized by HPCap program

To verify the validity of the coded analysis program, a comparative case was simulated using a well-known commercial program LPile which is also based on the finite-difference method. Analysis through the LPile program had been used since the early 1980s and is widely established in engineering practice. The parameters used for the comparative analysis between HPCap and LPile are listed in Table 2, in which Reese *et al.* (1974) *p-y* curve is used. A single steel pile with a diameter of 101.6 mm and 4 mm thickness is laterally loaded with the load applied at 0.2 m above ground level and embedded 3 m below with a total length of 3.2 m. The steel pile was assigned a yield strength of 355 Mpa and a modulus of elasticity equal to 210 GPa during the simulation. HPCap produced identical results with LPile in displacement, bending moment, shear, and soil resistance, as shown in Figs. 14(a)-14(d) respectively.

5.2 Modified p-multiplier and p-y springs concept

The original p-multiplier concept found in the studies conducted by Brown *et al.* (1988) and Fayyazi *et al.* (2012) was used as a reduction factor for piles acting in-group action. In this study, the p-multiplier accounts for the presence of the helices on the pile, not as a reduction but as a reinforcement factor, which is a function of effective helix diameter (difference between helix diameter and shaft diameter) and zone of influence. As shown in Fig. 15, the lateral resistance is offered not only by the shaft length and diameter but also by the additional soil resistance from the helix blades. Prasad and Rao (1996) first mentioned this in their study. With the application of lateral loads, the top and bottom faces of the helix resist the load in compression to the soil layer. It is hypothesized that the equilibrium of the forces acting on the helices will provide additional pile stiffness that will substantially decrease the lateral deflection of a helical pile compared to a normal pile.

Fig. 16 shows the difference between a single pile configuration with traditional *p-y* springs versus the proposed helical pile configuration with modified *p-y* springs. The traditional *p-y* springs are modified using the p-multiplier concept by introducing an adjustment factor displayed in Eq. (14) that accounts for the presence of the helices. The number of nodes in which the modified springs are applied depends on the zone of influence of a helix.

$$P_{mult} = \Omega\left(\frac{D_h - D_p}{D_p}\right) \tag{14}$$

where Ω is the pile coefficient, D_h is the helix diameter and D_p is the pile shaft diameter

5.3 Distribution of the p-y springs with modified p-multipliers

The distribution of the modified *p-y* springs is linear, with a maximum value near the center and gradually decreasing towards a minimum value bounded by the zone of influence, as shown in Fig. 16. The concept of the p-multiplier is to introduce an adjustment factor to the soil resistance in a typical *p-y* curve which modifies its base value, hence called p-multiplier as only the soil resistance is adjusted. That adjustment factor is not necessary for a laterally loaded single pile, so the value is, by default, 1.0. In the case of laterally loaded helical piles, the *p-y* springs are modified to account for the presence of helices; this results in an adjustment factor greater than 1.0. Now, the adjustment factor value depends on the empirical formula presented in this study, as shown in Eq. (14). The full value of the p-multiplier is applied to the spring at the center of the zone of influence (where the helix is located) which gradually decreases as it approaches the boundary of the zone of influence. The springs outside the influence zone are not modified, so the p-multiplier is unnecessary; therefore, its default value is 1.0. The minimum value of the *p*-multiplier is always 1.0 and not lesser as it would indicate loss of soil strength. The maximum value, however, is determined by the empirical formula.

In Table 2, D_p is the pile shaft diameter, t is the pile wall thickness, L is the total pile length, e is the exposed pile length above ground line, L_e is the embedded pile depth, ϕ is the peak friction angle from SPT, γ is the effective unit weight of soil, k_0 is the coefficient of earth pressure at rest, k_h is the initial modulus of subgrade reaction (which is a function of angle of the peak internal friction, see Eqs. (15(a) and 15(b)) and F_x is the lateral load applied at the pile head.

Table 2 Parameters for comparative case between HPCap and LPile

Parameter	Description/Value
D_p	101.6 mm
t	4.0 mm
L	3.2 m
e	0.2 m
L_e	3.0 m
ϕ	33.4°
γ	8.19 kN/m^3
k_0	0.4
k_h	function of ϕ
F_x	8.2 kN

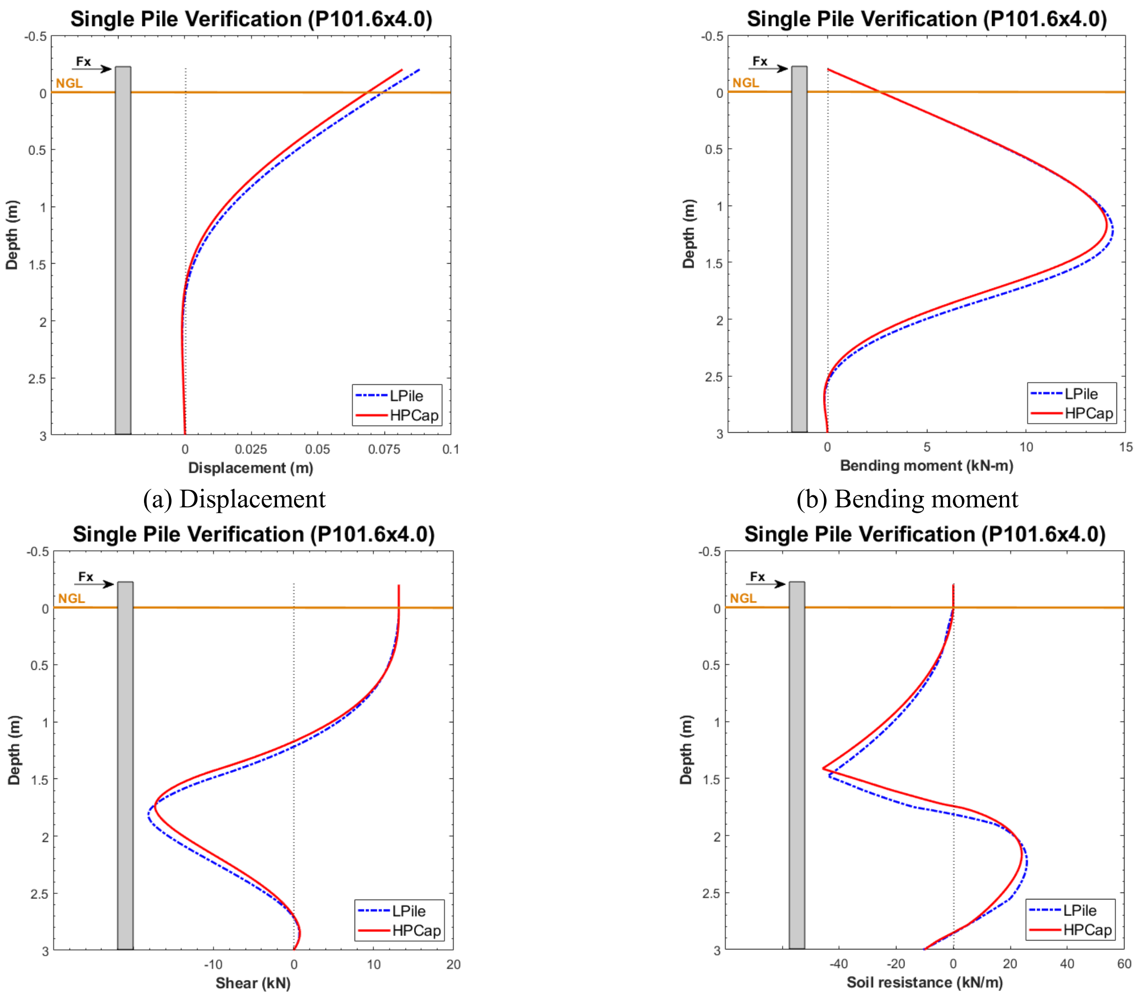

(a) Displacement (b) Bending moment

(c) Shear (d) Soil Resistance

Fig. 14 Comparative results between HPCap and LPile in establishing validity

For sand above the water table

$$k_h = 278.014(0.4168\phi^2 - 8.1254\phi - 83.664) \quad (15a)$$

For sand below the water table

$$k_h = 278.014\begin{pmatrix} 0.0166\phi^3 - 1.5526\phi^2 \\ +58.43\phi - 769.18 \end{pmatrix} \quad (15b)$$

5.4 Determination of pile coefficient and zone of influence

The pile coefficient and zone of influence are determined through linear regression of the best-fit values obtained from trial and error analysis. Selection of the best-fit values is based on the least percent error comparison from the conducted field tests versus the simulated numerical results. The process for determining the pile coefficient and zone of influence is reiterative. Since both the pile coefficient and zone of influence are unknown, the reiterative process becomes complex and requires an independent equation where the solution to one of the unknowns becomes feasible without the influence of the other; this results in a substantial amount of data to be analyzed. To minimize the extensive data collection for reiteration, four cases of the zone of influence are held as control variables, leaving the pile coefficient to be analyzed and fitted to the field results. After obtaining the best pile coefficients for each helical pile configuration, the zone of influence case is changed, and another set of pile coefficients is solved under the new zone of influence case.

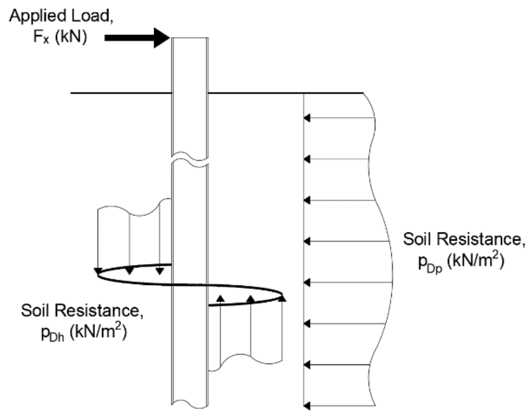

Fig. 15 Soil resistance concept for laterally loaded helical piles

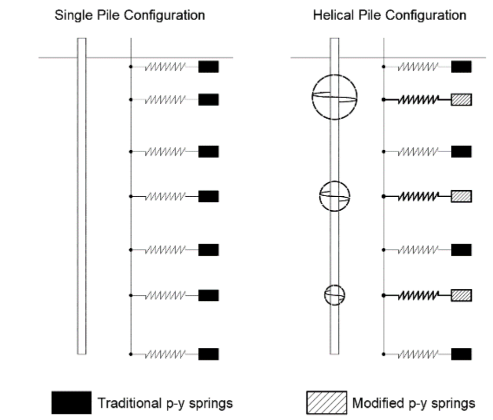

Fig. 16 Comparison between a single pile versus a helical pile *p-y* spring configuration

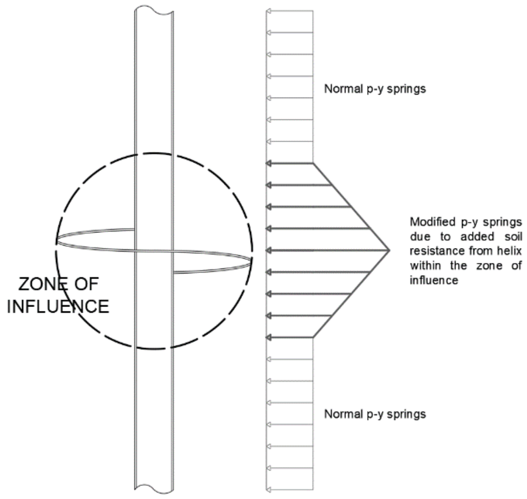

Fig. 17 Distribution of *p-y* springs for helical piles

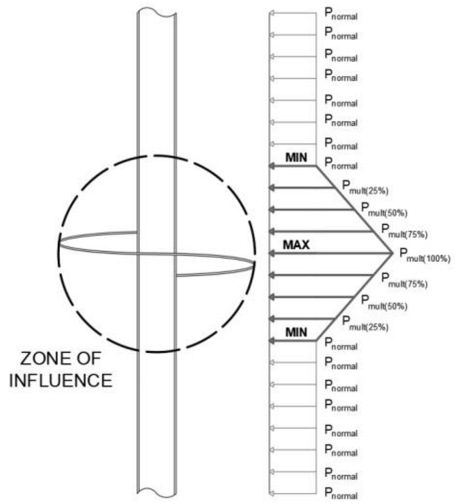

Fig. 18 Distribution of p-multipliers on the *p-y* springs for helical piles

The process flow is described in Fig. 19. When all four cases of the zone of influence are simulated and assigned with the best fit coefficients, linear regression is performed to find the trend of the three helical pile configurations (P89.1, P101.6, and P114.3) for each zone of influence case.

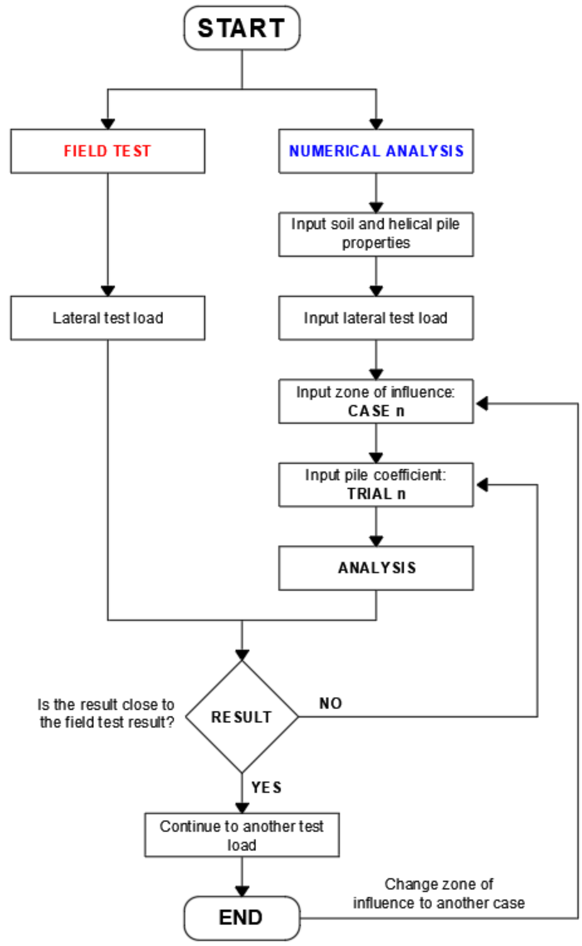

Fig. 19 Reiterative process flow for determination of pile coefficient and zone of influence

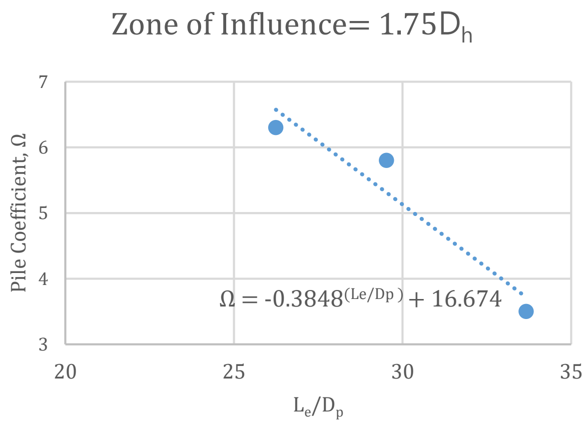

Fig. 20 Linear regression trend of the least percent error

Afterward, the trend equation is used to simulate the analysis, and another round of comparison between the field test data and the simulated results is done.

The smallest percentage of error is found using the zone of influence equal to 1.75D_h, and the pile coefficient formula is a function of the ratio of pile embedment over shaft diameter, as displayed in Eq. (16) and shown in Fig. 20.

5.5 Numerical analysis of helical piles using HPCap

After establishing the pile coefficient from Eq. (16) and determining the zone of influence as $1.75D_h$, the numerical analysis of laterally loaded helical piles can now be solved through the self-coded program. The HPCap program does not require the input of material yield strength, unlike LPile, since the objective of the program is to produce results based on the input parameters.

$$\text{pile coefficient } (\Omega) = -0.3848^{\left(\frac{L_e}{D_p}\right)} + 16.674 \quad (16)$$

where L_e is the length of pile shaft embedment and D_p is the diameter of pile shaft

To start the analysis, the input of pile properties is required, such as total pile length (embedded + exposed segment), the distance of pile head above ground level, pile diameter and thickness, steel modulus of elasticity, number of helices (location and helix diameter), these basic input parameters are required to establish the geometric configuration of the helical pile. Next is the input of soil properties; in this section, the user is required to define the soil layer height since the program can analyze up to five soil layers; once the height is specified, the soil properties can be inputted. The selection of the *p-y* curve is based on the soil classification. For this analysis, the *p-y* curve of Reese *et al*. (1974) was chosen. After selecting the *p-y* curve, the input parameters such as unit weight, friction angle, in-situ coefficient, and horizontal subgrade modulus will be required (note that not all input parameters are required as it depends on the soil type, whether sand or clay). With most geotechnical engineering-related problems, the analysis is only reliable as the soil parameters used; it is important to consider the presence of the water table in the soil layers, and effective soil parameters need to be used for layers below the water table. Once the pile properties and soil parameters are set, the program will display the helical pile configuration embedded in the soil layers. In the lateral analysis tab, the user is required to the input type of load, such as horizontal load or moment (at the top of pile head). In this case, to simulate the results from the conducted field tests, only the input of lateral load at the top of the pile head (during the field tests, the load was applied 0.2 m from the ground, but in the simulated analysis, the pile head is assigned to be 0.2 m above ground level to match the field conditions) is considered.

Once the analysis runs, the results are obtained after 30-45 seconds displaying the deflection at the top of the pile head, displacement at the ground level, and maximum bending moment developed along its entire length. The maximum bending moment result is essential for checking the capacity of the pile material and section and whether it is sufficient to withstand such magnitude. Additional results such as deflection, bending moment, slope (rotation of the pile from its initial position), shear, and soil resistance diagrams along the pile length are also accessible in the post-processing tabs.

Displayed in Figs. 21 to 23 are the displacements on the top of the pile head from field tests and simulated results. As shown, the numerical analysis results show slight over predicted results ranging from 1-2 mm, which is roughly 10-20% greater lateral capacity compared to the measured field test data; this could be attributed to installation effects as discussed in several studies as the soil medium is remolded due to the presence of helices.

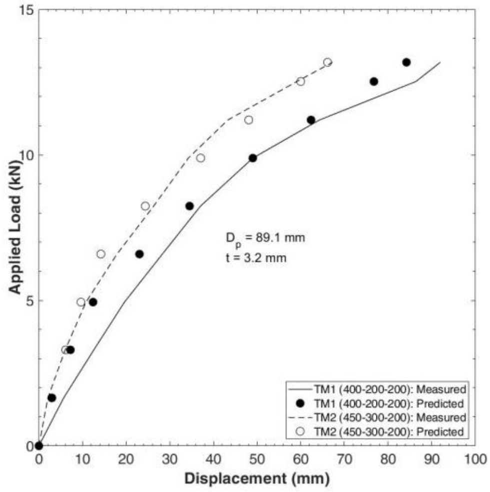

Fig. 21 Predicted versus field test data for TM1 & TM2

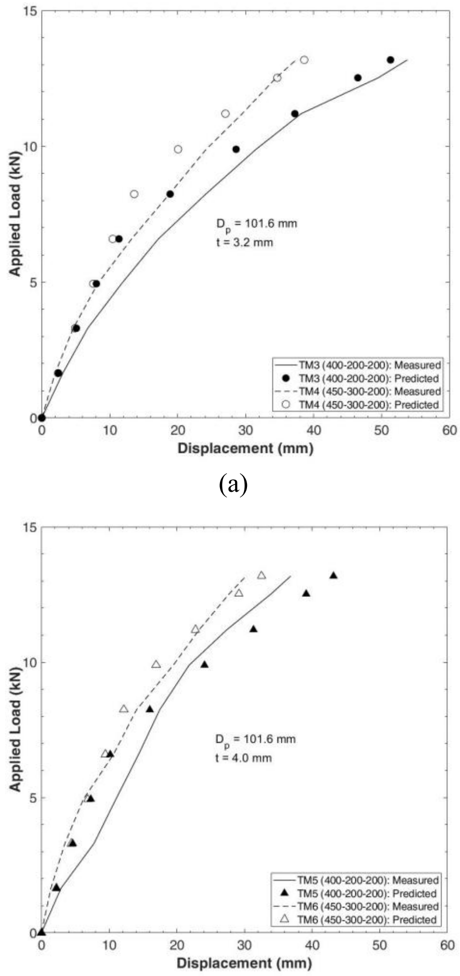

(a)

(b)

Fig. 22 Predicted versus measured data for piles with D_p = 101.6 mm a) TM3 & TM4 and (b) TM5 & TM6

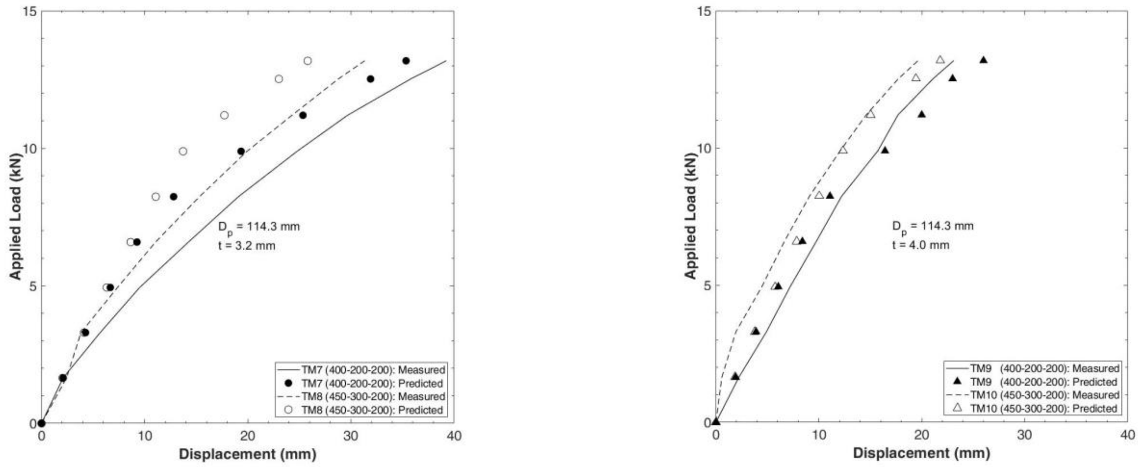

(a) (b)

Fig. 23 Predicted versus measured data for piles with D_p = 114.3 mm (a) TM7 & TM8 and (b) TM9 & TM10

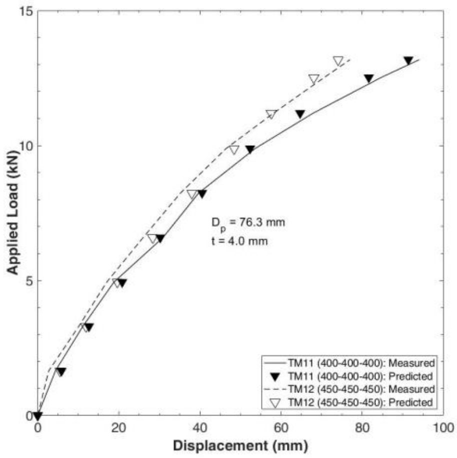

Fig. 24 Predicted versus field test data for pile with D_p = 76.3 mm

5.6 Verification of modified p-multipliers from another pile configuration

Two cases of laterally loaded helical piles were installed near the test bed labeled TB-2. The test piles have a shaft diameter of 76.3 mm and a thickness of 4.0 mm. Welded to the pile shaft are three helices with equal diameters. Case-11 has a 400-400-400 (measured in millimeters) helix configuration, while Case-12 has a 450-450-450 (measured in millimeters) helix configuration. The helical piles have a total length of 3.5 m, where 3m is embedded in the soil. The location of the first helix is 0.7 m below the ground, and succeeding helices are spaced 1m apart. The steel material for the helical pile has a yield strength of 355 MPa and a modulus of elasticity of 210 GPa. The test loads and soil properties are similar to the prior cases (see Sections 3 & 4).

The load-displacement graph for the P76.3 helical pile is shown in Fig. 24. The helical pile with helix configuration 450-450-450 exhibits lesser displacement than the 400-400-400 helix configuration, indicating greater lateral resistance compared to the latter. As shown in the figure, the predicted values from the numerical analysis agree with the measured field test results.

6. Conclusions

Presented in this study is the development of modified *p-y* curves to characterize the lateral behavior of helical piles embedded in reclaimed soils. A numerical method of analysis is proposed and demonstrated to account for the presence of helices attached to the central shaft of a single pile and its significance on the lateral resistance. The method is based on the theory of a Winkler foundation, an embedded pile element connected to the soil medium via non-linear springs supplemented by the concept of modified p-multipliers to account for the presence of helices around the central shaft. The *p-y* curves are modified along the embedded pile length to increase the stiffness of the areas under the zone of influence. The input soil properties are obtained and correlated from SPT-N in-situ tests. The soil unit weight used for analysis must be an effective unit weight to account for the presence of the water table.

Based upon the initial research findings are the following observations and key points on the behavior of a laterally loaded helical pile:

- The zone of influence of a helical plate appears to be 1.75 times the diameter of the helix plate
- The pile coefficient (Ω) which is a function of the ratio of pile embedment to pile diameter serves as a general fitting parameter for this research study
- The difference of 1-2 mm (which roughly corresponds to 10-20%) from the measured vs simulated data can potentially be attributed to possible installation effects
- The stiffness offered by the helical plate for the lateral resistance of a helical pile is dependent on the proposed p-multiplier distribution as shown in Fig. 18. With maximum stiffness offered at the central location of the helix position and linearly decreasing away from the center to a minimum value of one, which implies that the boundary of the zone of influence is reached.

The HPCap program, developed by the research laboratory of Kunsan National University, and based on the finite difference method, has its validity tested with the popular commercial software LPile. The program is capable of predicting the displacement, bending moment, shear, and soil resistance of laterally loaded helical piles and simulating multi-layered soils with different soil parameters and soil classification per layer.

The predicted lateral displacements of the various pile diameters generated through the numerical analysis show acceptable results compared to the recorded field test results.

Acknowledgements

The research presented by this paper was supported by the Basic Science Research Program through the National Research Foundation of Korea (NRF). Funded by the Ministry of Education (NRF2021R1A6A1A1A0304518511, NRF2020R1I1A3A04036506).

References

ASTM D3966-07: Standard Test Methods for Deep Foundations Under Lateral Load.

Abdrabbo, F.M. and El Wakil, A.Z. (2016), “Laterally loaded helical piles in sand”, *Alexandria Eng. J.*, **55**(4), 3239-3245. https://doi.org/10.1016/j.aej.2016.08.020.

Al-Baghdadi, T., Brown, M.J., Knappett, J.A. and Ishikura, R. (2015), “Modelling of laterally loaded screw piles with large helical plates in sand”, *Proceedings of the 3rd Int. Symp. On Frontiers in Offshore Geotechnics*, Oslo, Norway. 10-12 June 2015. Taylor & Francis Group, London.

Al-Baghdadi, T., Brown, M.J., Knappett, J.A. and Humaish, A. (2017), “Effects of vertical loading in lateral screw pile performance”, *Proc. Inst. Of Civil Engineers: Geotech. Eng. J.*, **170**, 259-272. http://dx.doi.org/10.1680/jgeen.16.00114.

Bouzid, D.A., Bhattacharya, S. and Dash, S.R. (2013), “Winkler springs (*p-y curves*) for pile design from stress-strain soils: FE assessment of scaling coefficients using the mobilized strength design concept”, *Geomech. Eng.*, **5**(5), 379-399. https://doi.org/10.12989/gae.2013.5.5.379.

Brown, D.A., Morrison, C. and Reese, L.C. (1988), “Lateral load behavior of pile group in sand”, *J. Geotech. Eng.*, **114**(11), 1261-1276. https://doi.org/10.1061/(ASCE)0733-9410(1988)114:11(1261).

Cheng, Z. and Jeremic, B. (2009), “Numerical modeling and simulation of soil lateral spreading against piles”, *Proc., Int. Foundation Congress and Equipment Expo*, Vol. 1, ASCE, Reston, VA.

Crowther, S.G. (1990), “Analysis of laterally loaded piles embedded in layered frozen soil”, *J. Geotech. Eng.*, **116**(7), 1137 https://doi.org/10.1061/(ASCE)0733-9410(1990)116:7(1137).

Davidson, C., Brown, M.J., Cerfontaine, B., Al-Baghdadi, T., Knappett, J., Brennan, A. and Ball, J.D. (2022), “Physical modelling to demonstrate the feasibility of screw piles for offshore jacket-supported wind energy structures”, *Géotechnique*, **72**(2), 108-126. https://doi.org/10.1680/jgeot.18.P.311.

Dobry, R., Abdoun, T., O’Rourke, T.D. and Gosh, S.H. (2003), “Single piles in lateral spreads: Field bending moment evaluation”, *J. Geotech. Geoenviron. Eng.*, **129**(10), 879-889. https://doi.org/10.1061/(ASCE)1090-0241(2003)129:10(879).

Elkasabgy, M. and El Naggar, M.H. (2019), “Lateral performance and *p-y* curves for large-capacity helical piles installed in clayey glacial deposit”, *J. Geotech. Geoenviron. Eng.*, **145**(10). https://doi.org/10.1061/(ASCE)GT.1943-5606.0002063.

Fayyazi, M., Taiebat, M., Finn, W.D. and Ventura, C. (2012), “Evaluation of p-multiplier method for performance based design of pile groups”, *Proceings of the 2nd International Conference on Performance-Based Design in Earthquake Geotechnical Engineering*, Taormina, Italy, May.

Finn, W.D. and Thavaraj, T. (2001), “Deep foundations in liquefiable soils: case histories, centrifuge tests and method of analysis”, *Proceedings of the 4th Int. Conf. on Recent Advances in Geotechnical Earthquake Engineering and Soil Dynamics*, S. Prakash, ed., Univ. of Missouri, Rolla, MO, Paper No. SOAP-1.

Foriero, A., St-Laurent, N. and Ladanyi, B. (2005), “Laterally loaded pile study in permafrost of northern Quebec, Canada”, *J. Cold Reg. Eng.*, **19**(3), 61. https://doi.org/10.1061/(ASCE)0887-381X(2005)19:3(61).

Gleser, S.M. (1953), “Lateral load tests on fixed-head and free-head piles”, Special Technical Publication 154, 75-101, American Society for Testing Materials, Philadelphia, Pa.

Gonzales, L., Abdoun, T. and Doubry, R. (2005), “Effect of soil permeability on centrifuge modeling of pile response to lateral spreading”, *Proceings of the Seismic Performance and Simulation of Pile Foundations in Liquefied and Laterally Spreading Ground*, ASCE, Reston, VA, 50-60.

Haigh, S.K. (2002), “Effects of liquefaction on pile foundations in sloping ground”, Ph.D. dissertation, Cambridge University, Cambridge, U.K.

Haigh, S.K. and Madabhushi, S.P.G. (2002), “Centrifuge modeling of lateral spreading past pile foundations”, *Proceings of the Int. Conf. on Physical Modelling in Geotechnics*, ISSMGE, London, U.K.

Hatanaka, M. and Uchida, A. (1996), “Empirical correlation between penetration resistance and internal friction angle of sandy soils”, *Soils Found.*, **36**(4), 1-9. https://doi.org/10.3208/sandf.36.4_1.

He, L., Elgamal, A., Abdoun, T., Abe, A., Dobry, R., Hamada, M., Menses, J., Sato, M., Shantz, T. and Tokimatsu, K. (2009), “Liquefaction-induced lateral load on pile in a medium D_r sand layer”, *J. Earthq. Eng.*, **13**(7), 916-938. https://doi.org/10.1080/13632460903038607.

Hetenyi, M. (1946), “Beams on elastic foundation”, Scientific Series, vol. XVI. Ann Arbor: The University of Michigan Press, University of Michigan Studies.

Japan Road Association (2002), *Specifications for highway bridges*, Japan Road Association, Tokyo, Japan.

Kim, H.J., Kim, H.S., Park, T.W., Dinoy, P.R., Kim, J.Y. and Reyes, J.V. (2020), “Liquefaction Prediction of Saemangeum Silty Sand using LiqAS Program”, *ACEM20*, Seoul, Korea.

Kim, H.J., Park, T.W., Dinoy, P.D. and Kim, H.S. (2021), "Performance and design of modified geotextile tubes during filling and consolidation", *Geosynthetics Int.*, **28**(2), 125-143. https://doi.org/10.1680/jgein.20.00035.

Kim, G., Kyung, D., Park, D. and Lee, J. (2015), "CPT-based *p-y* analysis for mono-piles in sands under static and cyclic loading conditions", *Geomech. Eng.*, **9**(3), 313-328. https://doi.org/10.12989/gae.2015.9.3.313.

Kulhawy, F.H. and Mayne, P.W. (1990), *Manual on estimating soil properties for foundation design* (No. EPRI-EL-6800). Electric Power Research Inst., Palo Alto, CA (USA); Cornell Univ., Ithaca, NY (USA). Geotechnical Engineering Group.

Lam, I., Arduino, P. and Mackenzie-Helnwein, P. (2009), "OPENSEES soil-pile interaction study under lateral spread loading", *Proceediings of the Int. Foundation Congress and Equipment Expo*, Vol. 1, ASCE, Reston, VA, 206-213.

Lee, M.J., Bae, K.T., Lee, I.W. and Yoo, M.T. (2019), "Cyclic *p-y* curves of monopiles in dense dry sand using centrifuge model tests", *MDPI: Appl. Sci.,* **9**(8), 1641. https://doi.org/10.33 90/app9081641.

Li, Q. and Yang, Z. (2017), "*p-y* approach for laterally loaded piles in frozen silt", *J. Geotech. Geoenviron. Eng.*, **143**(5). https:// doi.org/10.1061/(ASCE)GT.1943-5606.0001556

Li, X.S. and Dafalias, Y.F. (2000), "Dilatancy for cohesionless soils", *Geotechnique*, **50**(4), 449-460. https://doi.org/10.1680/ geot.2000.50.4.449.

Lim, H. and Jeong, S. (2018), "Simplified *p-y* curves under dynamic loading in dry sand", *Soil Dyn. Earthq. Eng.*, **113**, 101-111. https://doi.org/10.1016/j.soildyn. 2018.05.017.

LPile v (2019), Technical Manual, Ensoft Inc.

Lutenegger, A.J. (2011), "Historical development of iron screw-pile foundations: 1836-1900", *Int. J. History Eng. Tech.*, **81**(1), 108-128. https://doi.org/10.1179/175812109X1254 7332391989.

Matlock, H. (1970), "Correlations for design of laterally loaded piles in soft clay", *Proceedings of the 2nd Offshore Technology Conference*, Houston, Texas, 22-24 April.

Matlock, H. and Reese, L.C. (1960), "Generalized solutions for laterally loaded piles", *J. Soil Mech. Found. Div. Am. Soc. Civil Engineers*, **86**(5), 63-91.

Mittal, S., Ganjoo, B. and Shekhar, S. (2010), "Static equilibrium of screw anchor pile under lateral loads in sands", *Geotech. Geol. Eng.*, **28**(5), 717-725. https://doi.org/10.1007/s10706-010-9342-4

Prasad, Y.V.S. and Rao, S. (1996), "Lateral capacity of helical piles in clays", *J. Geotech. Eng.*, **122**(11), 938-941.

Reese, L.C. and Matlock, H. (1956), "Non-dimensional solutions for laterally loaded piles with soil modulus assumed proportional to depth", *Proceedings of the Eight-Texas Conference on Soil Mechanics and Foundation Engineering*, Austin, Texas.

Reese, L.C., Cooley, L.A. and Radhakrishnan, N. (1984), "Laterally Loaded Piles and Computer Program COM624G", Technical Report K-84-2.

Reese, L.C., Cox, W.R. and Koop, F.D. (1974), "Analysis of laterally loaded piles in sand", Paper No. OTC 2312, *Proceedings of the 7th Offshore Technology Conference*, Houston, Texas.

Reese, L.C. (1997), "Analysis of laterally loaded piles in weak rock", *J. Geotech. Geoenviron. Eng.*, **123**(11), 1010. https://doi. org/10.1061/(ASCE)1090-0241(1997)123:11(1010)

Sakr, M. (2009), "Lateral resistance of high capacity helical piles—case study", Almita Manufacturing Ltd., Ponoka, Alberta, Canada.

Sakr, M. (2018), "Performance of laterally loaded helical piles in clayey soils established from field experience", *DFI J. Deep Found. Inst.,* **12**(1), 1937-5247. https://doi.org/10.1080/19375247.2018.1430481.

Shelman, A., Tantalla, J., Sritharan, S., Nikolaou, S. and Lacy, H. (2014), "Characterization of seasonally frozen soils for seismic design of foundations", *J. Geotech. Geoenviron. Eng.*, **140**(7). https://doi.org/10.1061/(ASCE)GT.1943-5606.0001065.

Spagnoli, G. and Gavin, K. (2015), "Helical piles as a novel foundation system for offshore piled facilities", SPE-177604-MS. Society of Petroleum Engineers. https://doi.org/10.2118/ 177604-MS

Vignesh, V. and Mayakrishnan, M. (2020), "Design parameters and behavior of helical piles in cohesive soils-A review", *Arabian J. Geosci.*, **13**(22). https://doi.org/10.1007/s12517-020-06165-1.

Welch, R.C. and Reese, L.C. (1972). "Laterally loaded behavior of drilled shafts", Research Report No. 89-10, conducted for Texas Highway Department and U.S. Department of Transportation, Federal Highway Administration Bureau of Public Roads, by Center for Highway Research, University of Texas at Austin, Austin, Texas.

Yang, Z., Elgamal, A. and Parra, E. (2003), "Computational model for cyclic mobility and associated shear deformation", *J. Geotech. Geoenviron. Eng.*, **129**(12), 1119-1127. https://doi.org/10.1061/ (ASCE)1090-0241(2003)129:12(1119).

Zhang, D. (1999), "Predicting capacity of helical screw piles in Alberta soils". M.Sc. thesis, Department of Civil and Environmental Engineering, University of Alberta, Edmonton, Alberta.

Zhang, D.J.Y., Chalaturnyk, R., Robertson, P.K., Sego, D.C. and Cyre, G. (1998), "Screw anchor test program (Part I): instrumentation, site characterization and installation", Department of Civil and Environmental Engineering, University of Alberta, Edmonton, AB.

JS